Aerospace Technology Congress 2019
Swedish Society of Aeronautics and Astronautics (FTF)

FAULT DETECTION AND ISOLATION BASED ON BOND GRAPH MODELS: APPLICATION TO AN ELECTROMECHANICAL ACTUATOR

Gabriel S. Sobral and Luiz C. S. Góes
Department of Mechanical Engineering
Instituto Tecnológico de Aeronáutica (ITA)
São José dos Campos, SP/Brazil

8-9 October 2019, Stockholm, Sweden

AGENDA

01. Introduction
    Research Motivation and Objectives

02. Fault Detection and Isolation

03. Electromechanical Actuator Model

04. Diagnostic Bond Graph Model

05. Simulation and Results
    Conclusions


Engines
(thrust reverser, inlet guide, vanes)
Slats
Spoilers
Flaps
Ailerons
Landing Gears
(doors, extension/retraction, locks, steering, brakes)
Elevators
Trim Horizontal Stabilizer
Rudder
E190-E2
E2

CONVENTIONAL AIRCRAFT POWER DISTRIBUTION

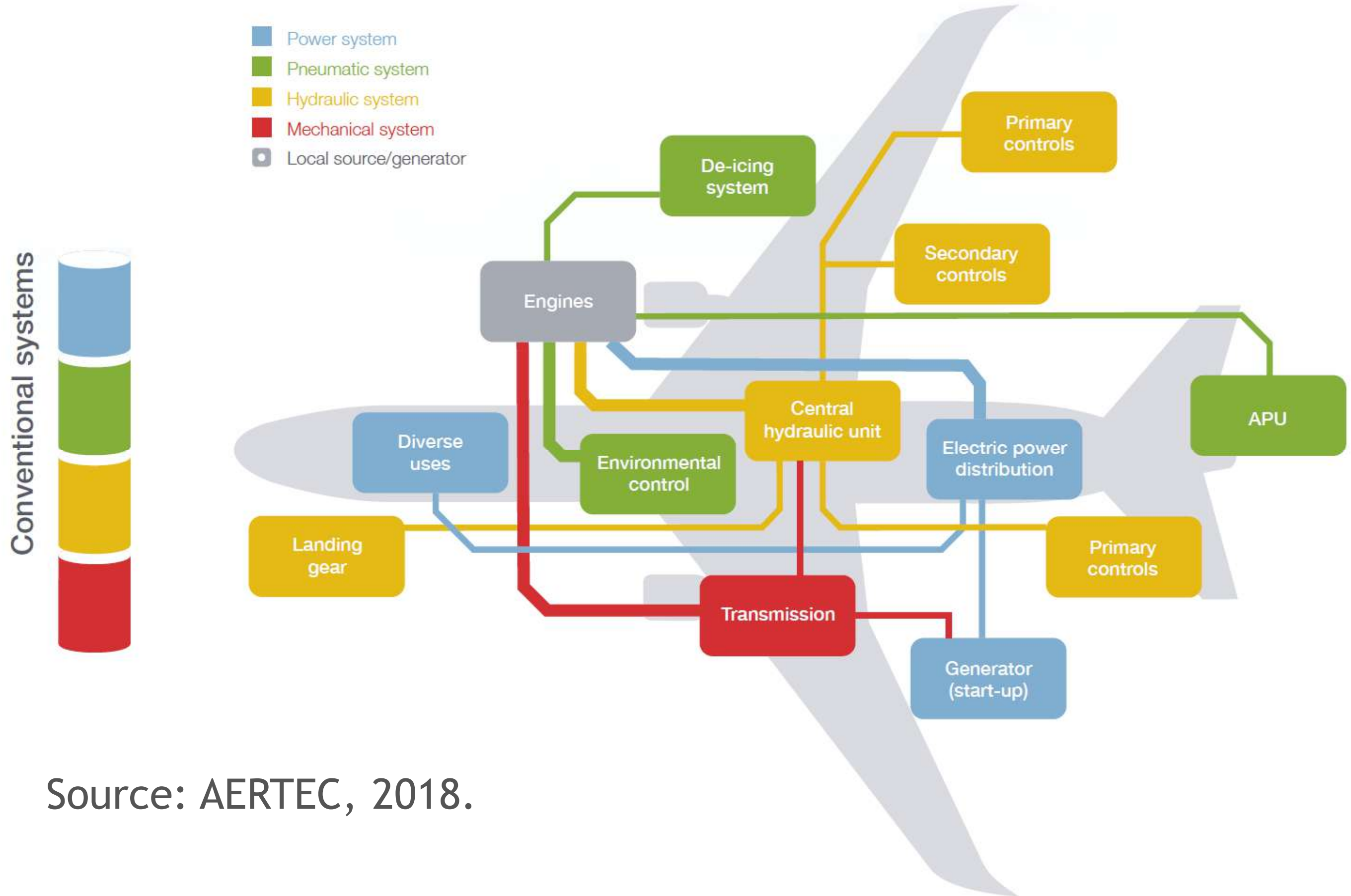

Source: AERTEC, 2018.

MORE ELECTRIC AIRCRAFT POWER DISTRIBUTION

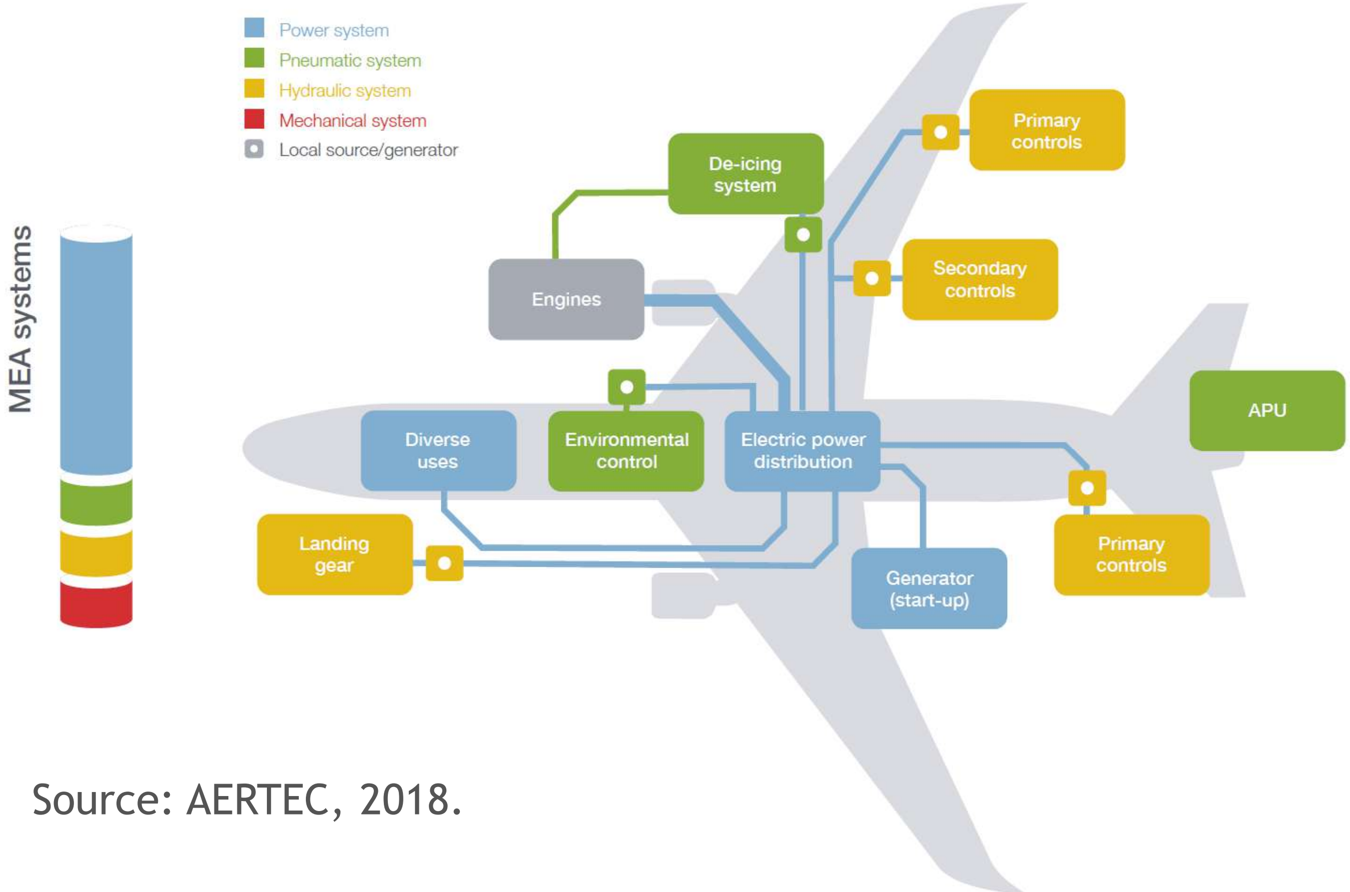

Source: AERTEC, 2018.

ELECTROMECHANICAL ACTUATOR (EMA)

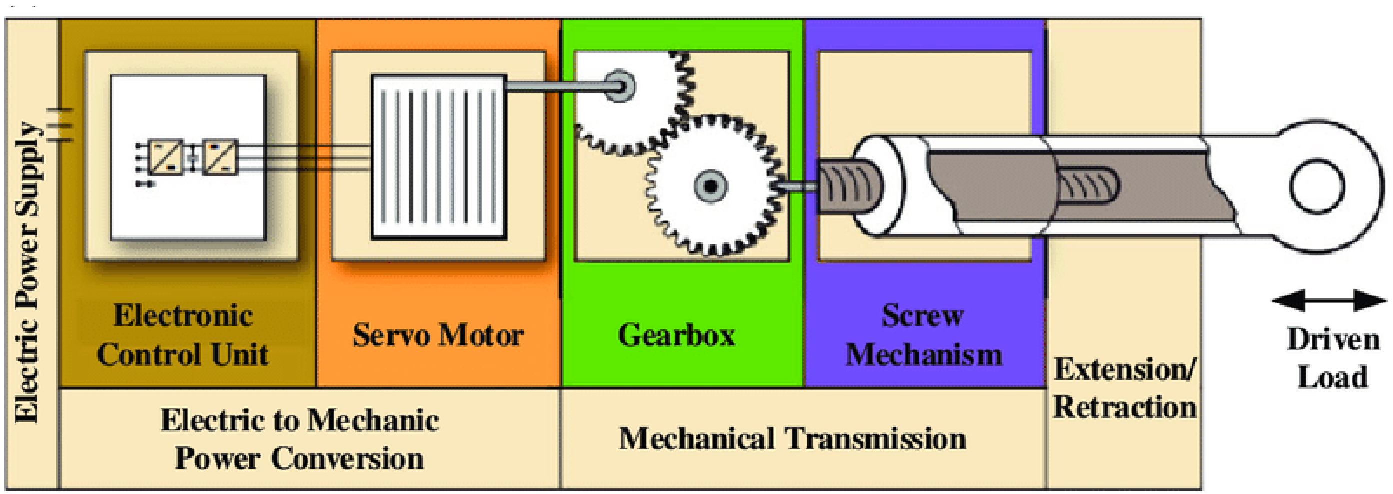

Source: QIAO et al., 2017.

RESEARCH MOTIVATION

- Industry trend towards power-by-wire actuators with evolution of the More Electric Aircraft concept
- Lack of accumulated knowledge and experience regarding EMA reliability and the risk of failures

RESEARCH MOTIVATION

- Industry trend towards power-by-wire actuators with evolution of the More Electric Aircraft concept
- Lack of accumulated knowledge and experience regarding EMA reliability and the risk of failures

RESEARCH OBJECTIVES

- Study and implementation of a quantitative model-based fault detection and isolation methodology based on bond graph
- Application to an EMA model

FAULT DETECTION AND ISOLATION

FAULT DEFINITION

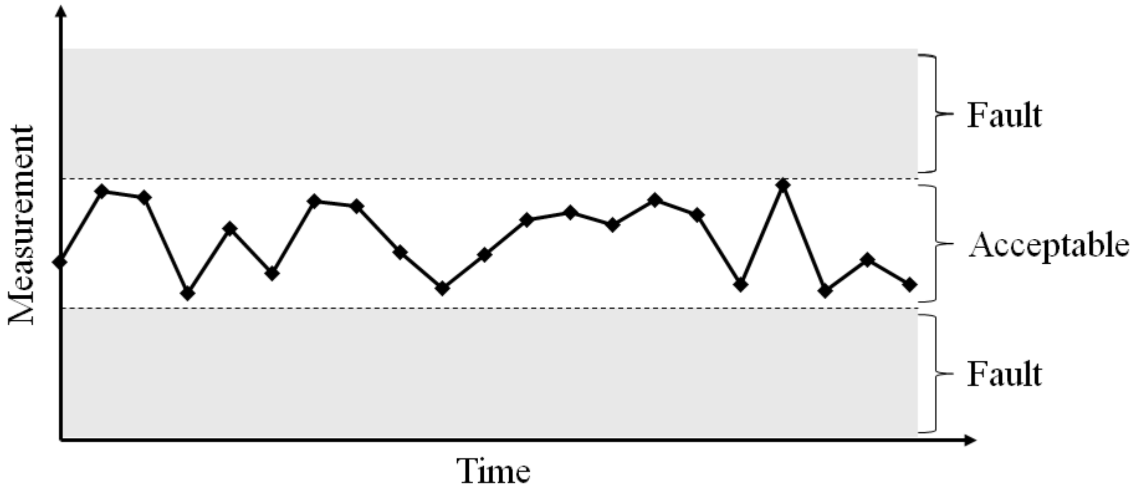

"**<u>Fault</u>** is generally defined as a departure from an acceptable range of an observed variable or a calculated parameter associated with a process." (VENKATASUBRAMANIAN et al., 2003)

FAULT DETECTION AND ISOLATION (FDI)

Fault detection: to determine if the system behavior has departed from the acceptable operation, raising a fault alarm in case of unacceptable behavior.

Fault isolation: to reduce the number of fault candidates, using one or more decision procedures to isolate the component responsible for the faulty behavior.

FAULT DETECTION AND ISOLATION (FDI)

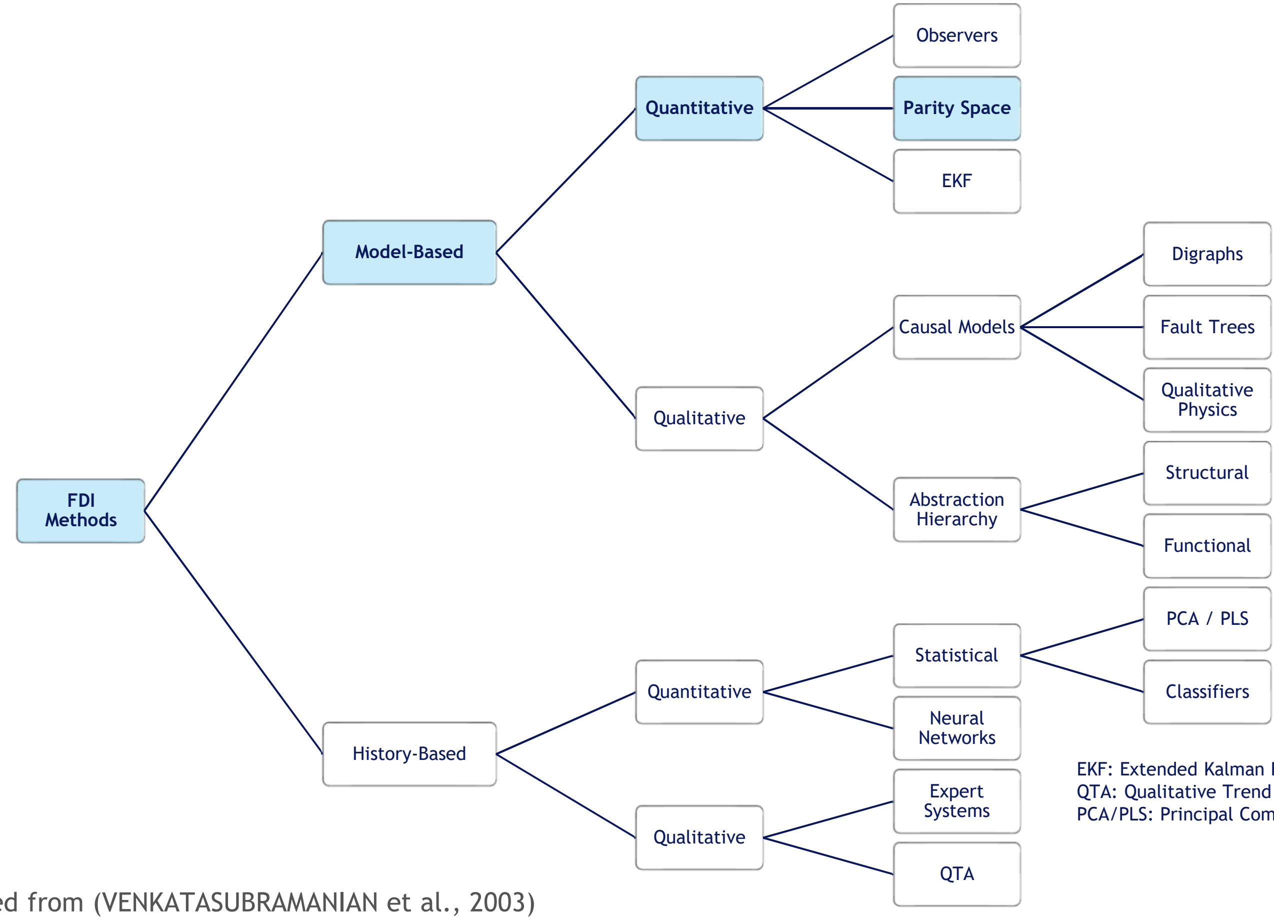

EKF: Extended Kalman Filter
QTA: Qualitative Trend Analysis
PCA/PLS: Principal Components Analysis/Partial Least-Squares

Source: adapted from (VENKATASUBRAMANIAN et al., 2003)

RESIDUAL SPACE MODEL-BASED FDI

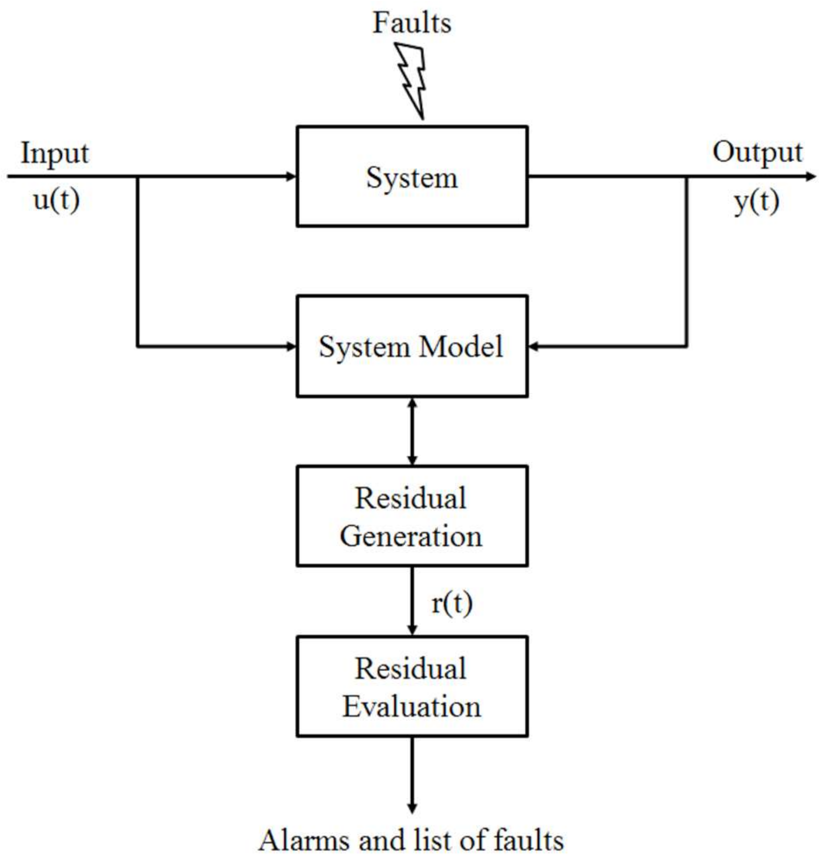

RESIDUAL SPACE MODEL-BASED FDI

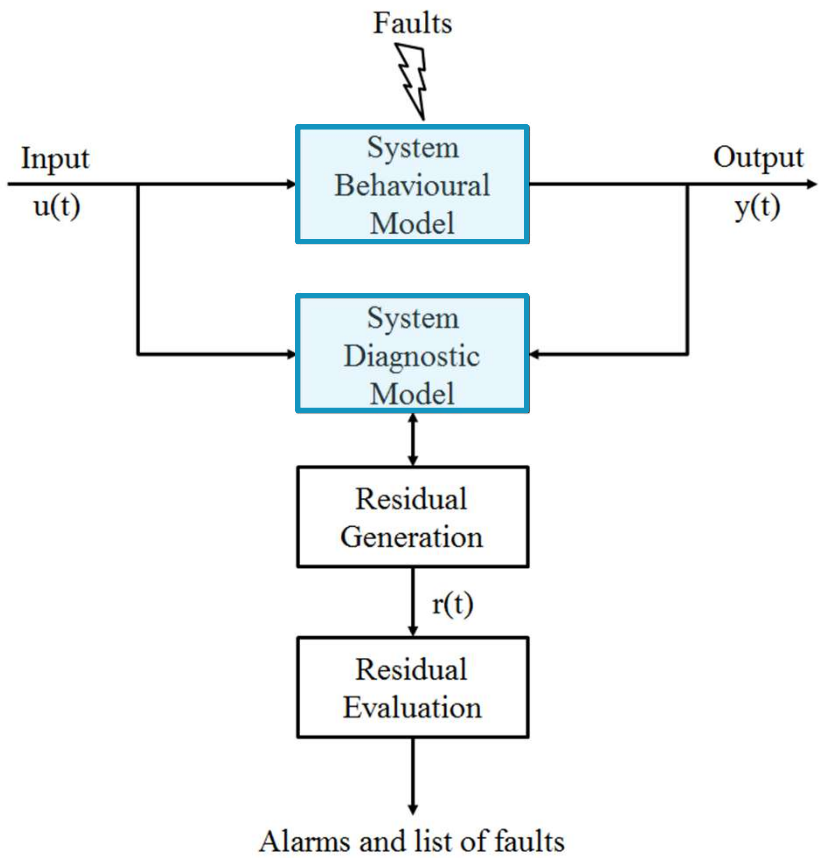

ELECTROMECHANICAL ACTUATOR MODEL

DIRECT DRIVE EMA

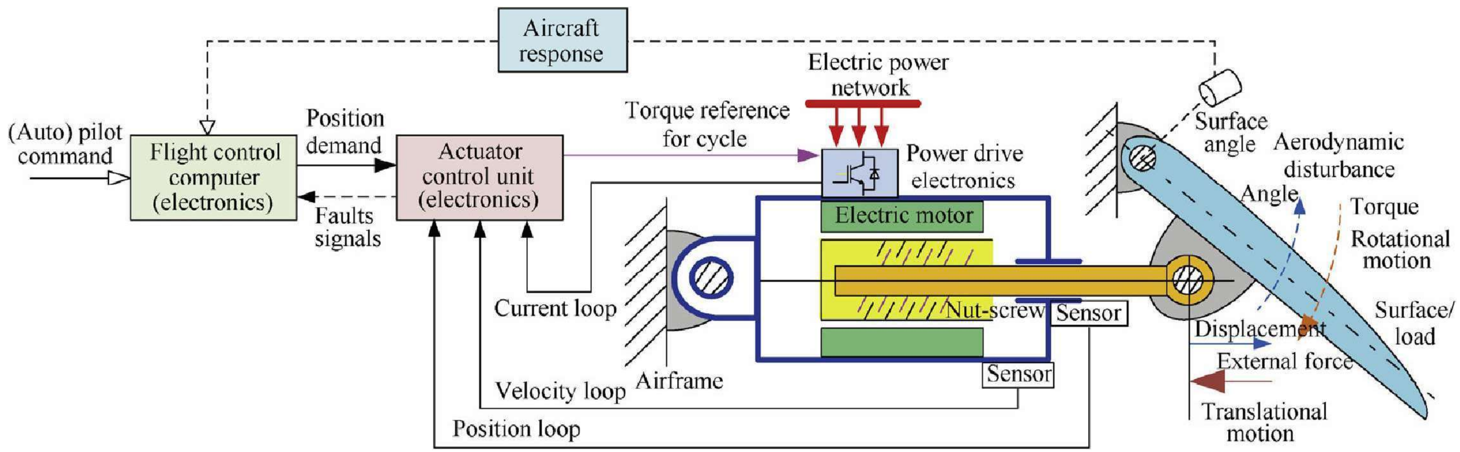

Source: FU et al., 2018.

DIRECT DRIVE EMA

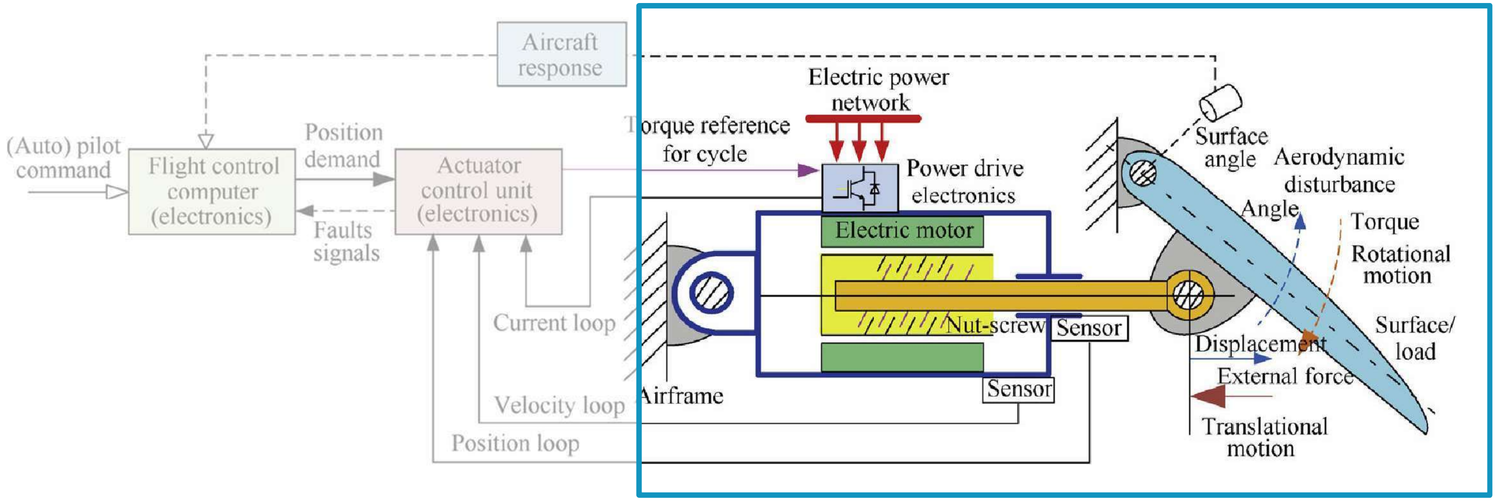

DIRECT DRIVE EMA – WORD BOND GRAPH

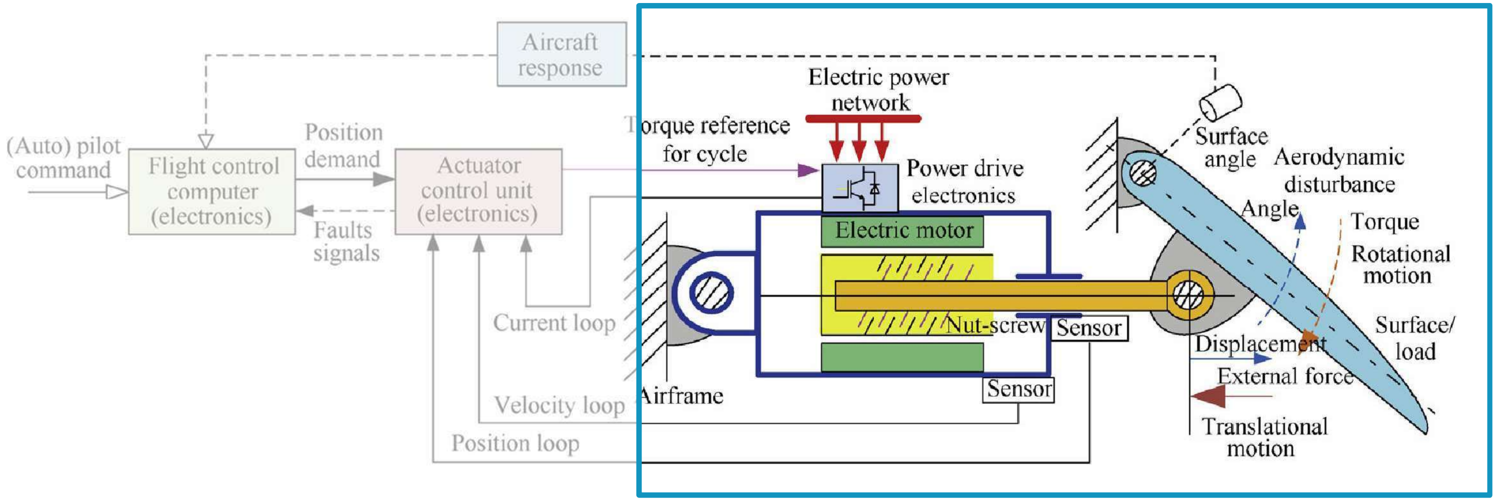

EM: Electric Motor

MPT: Mechanical Power Transmission

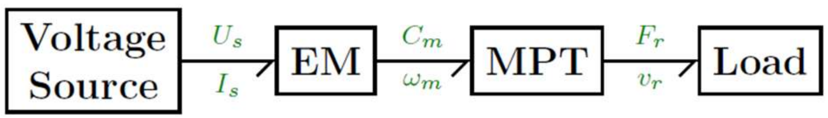

EMA BEHAVIOURAL MODEL

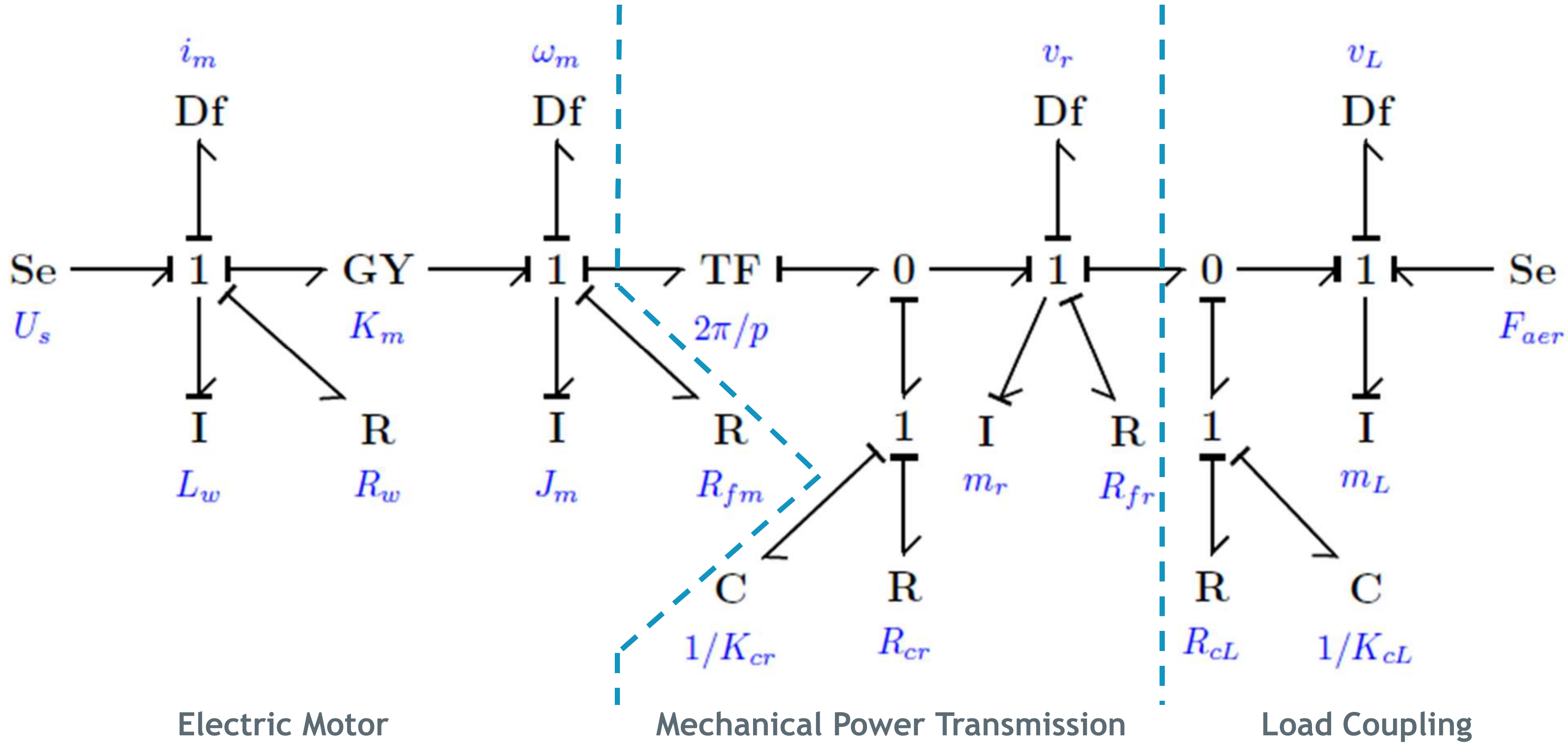

EMA FAILURE MODES

Short-circuit
Open-circuit

EM stator winding insulation deterioration, wire chafing, permanent winding failure.

Fault injection:

EM stator winding resistance

Backlash

MPT Excessive wear leading to backlash, or lost-motion.

Fault injection:

MPT compliance model

Jamming

MPT Increased friction, structural failure.

Fault injection:

MPT viscous friction coefficient

Free-play

Load coupling broken mechanical linkage.

Fault injection:

Load coupling contact force

DIAGNOSTIC BOND GRAPH MODEL

DIAGNOSTIC BOND GRAPH

- BG behavioural model with preferred differential causality
- Inversion of sensor causalities, i.e. sensors become sources
- Introduction of residual virtual sensors

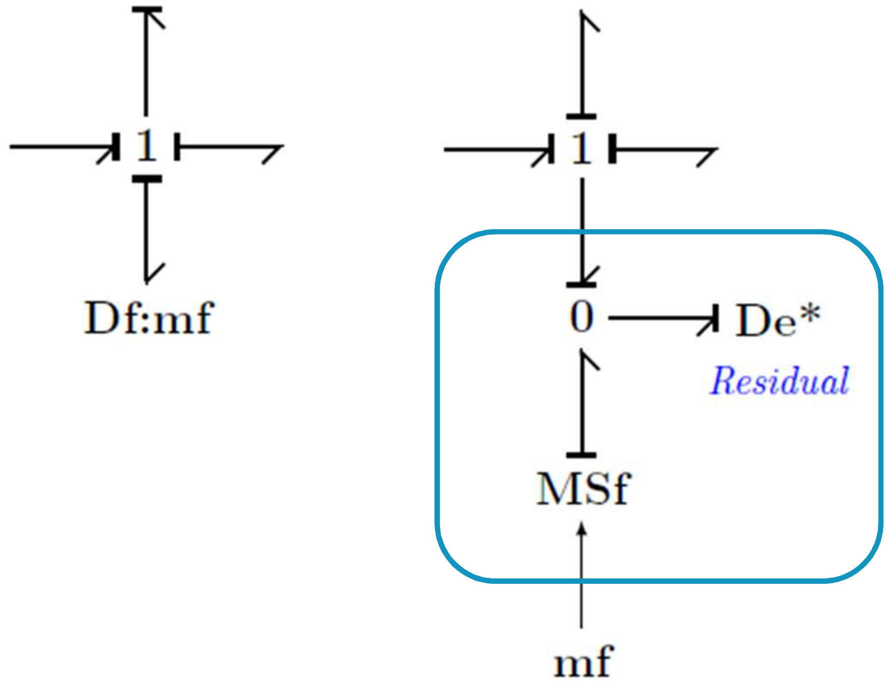

EMA DIAGNOSTIC BOND GRAPH

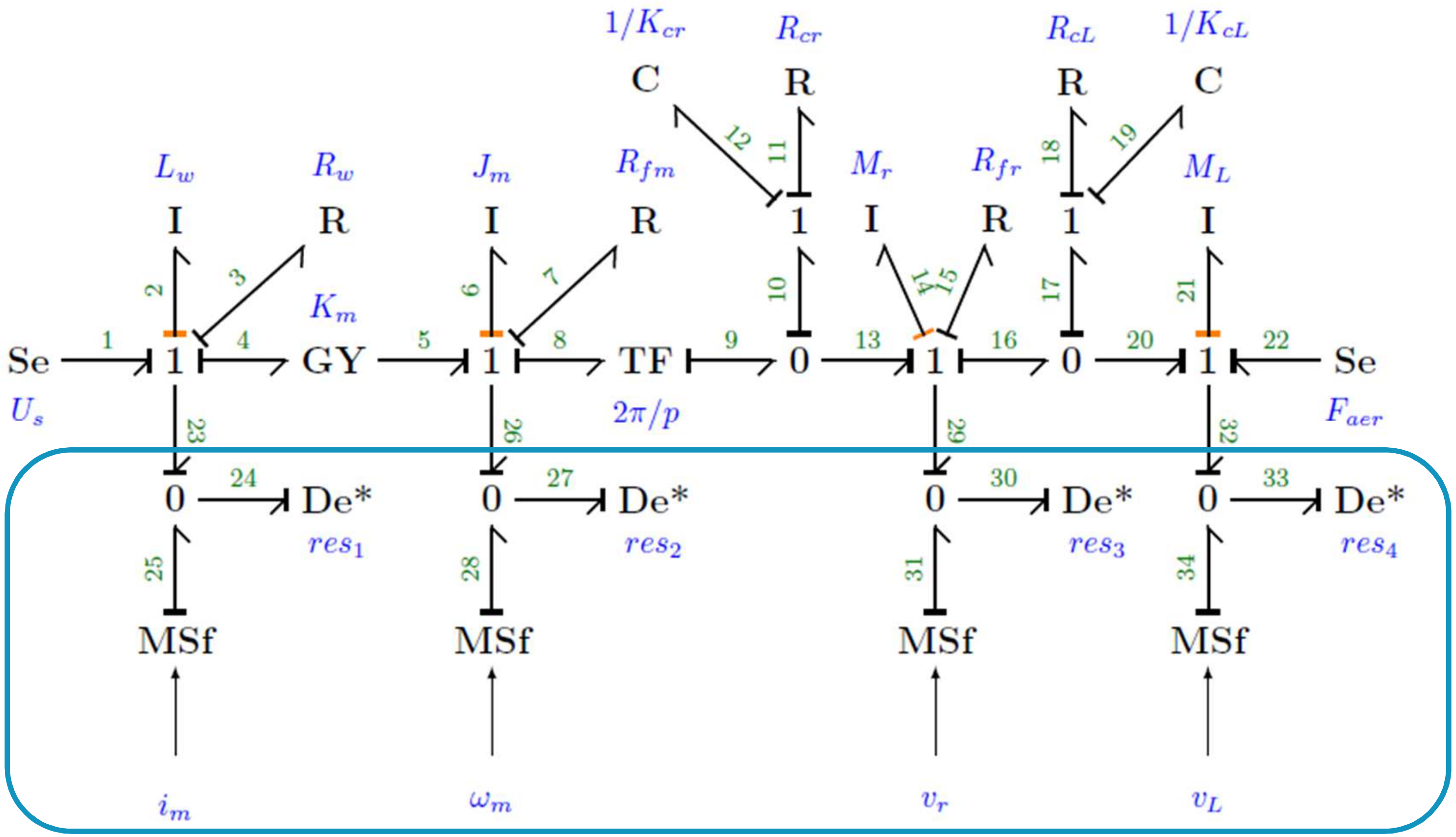

residual virtual sensors or **residual sinks**

EMA COUPLED MODELS

Diagnostic BG model

Coupling with noise injection

Behavioural BG model with fault injection

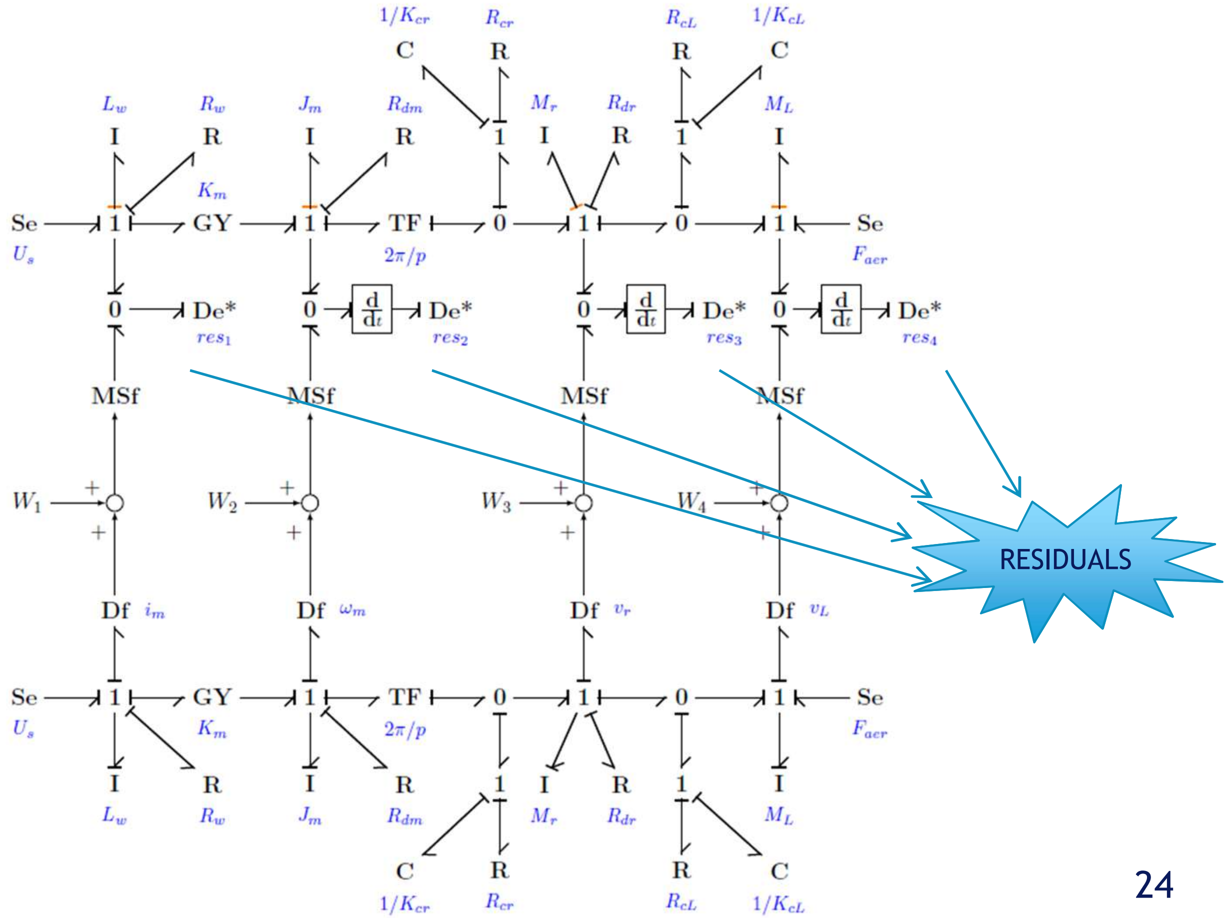

EMA FAULT SIGNATURE MATRIX

Subsystem	Component	res_1	res_2	res_3	res_4	D	I
EM electrical part	U_s	1	0	0	0	1	0
	L_w	1	0	0	0	1	0
	R_w	1	0	0	0	1	0
EM mechanical part	K_m	1	1	0	0	1	0
	J_m	0	1	0	0	1	0
	R_{fm}	0	1	0	0	1	0
MPT roller-screw	p	0	1	1	0	1	0
	R_{cr}	0	1	1	0	1	0
	K_{cr}	0	1	1	0	1	0
	M_r	0	0	1	0	1	0
	R_{fr}	0	0	1	0	1	0
Load coupling	R_{cL}	0	0	1	1	1	0
	K_{cL}	0	0	1	1	1	0
Load	M_L	0	0	0	1	1	0
	F_{aer}	0	0	0	1	1	0
Sensors	i_m	1	1	0	0	1	0
	ω_m	1	1	1	0	1	1
	v_r	0	1	1	0	1	0
	v_L	0	0	1	1	1	0

- Analysis of the causal paths leading to each residual detector
- Detectability index (D) of a component is set to 1 if at least one residual is sensitive to it
- Isolability index (I) is set to 1 when the component's fault signature is different from fault signatures of all other components

SIMULATION AND RESULTS

20-SIM BG MODEL IMPLEMENTATION

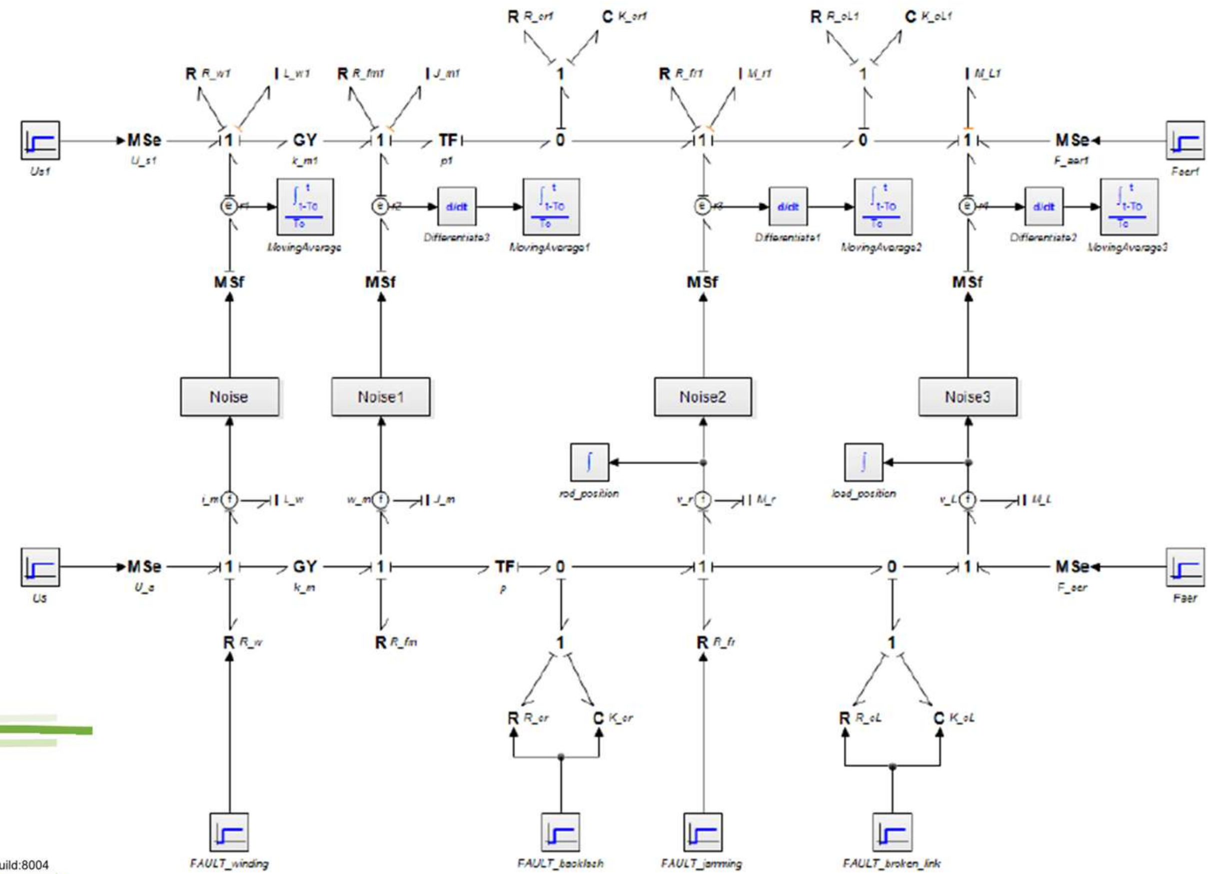

20-SIM
Version 4.6
4.6.4 build:8004

NORMAL OPERATION

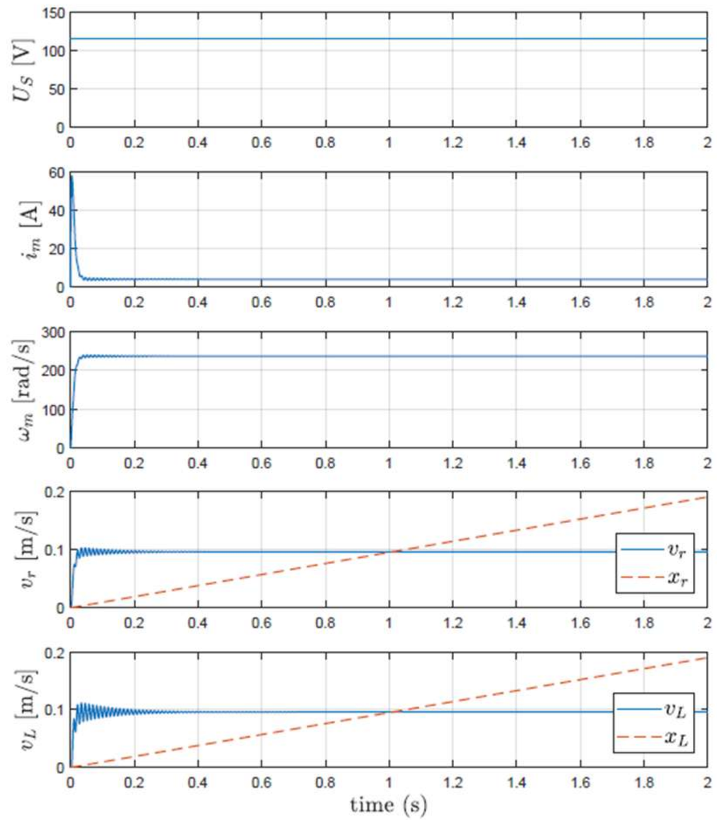

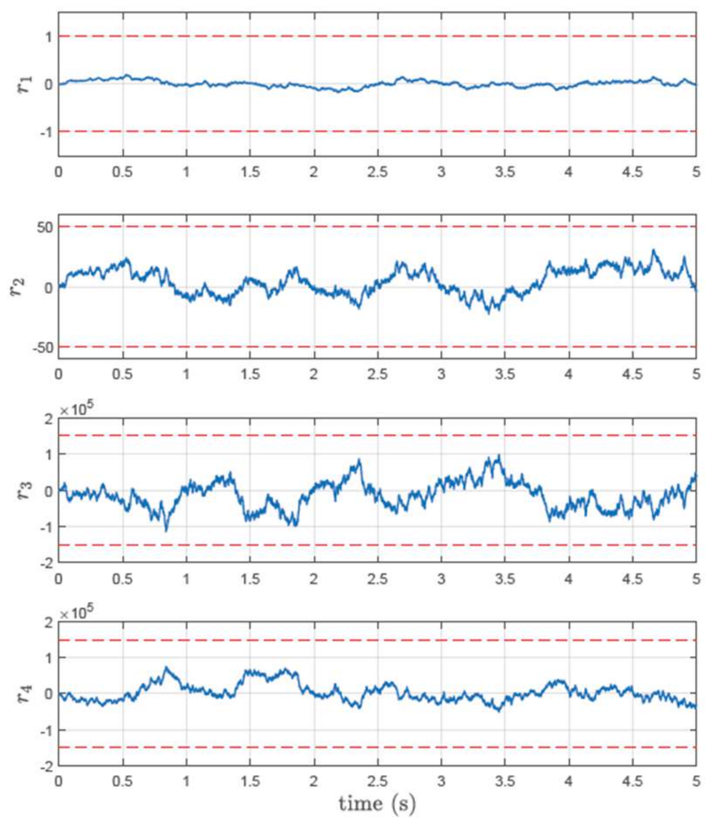

SHORT-CIRCUIT

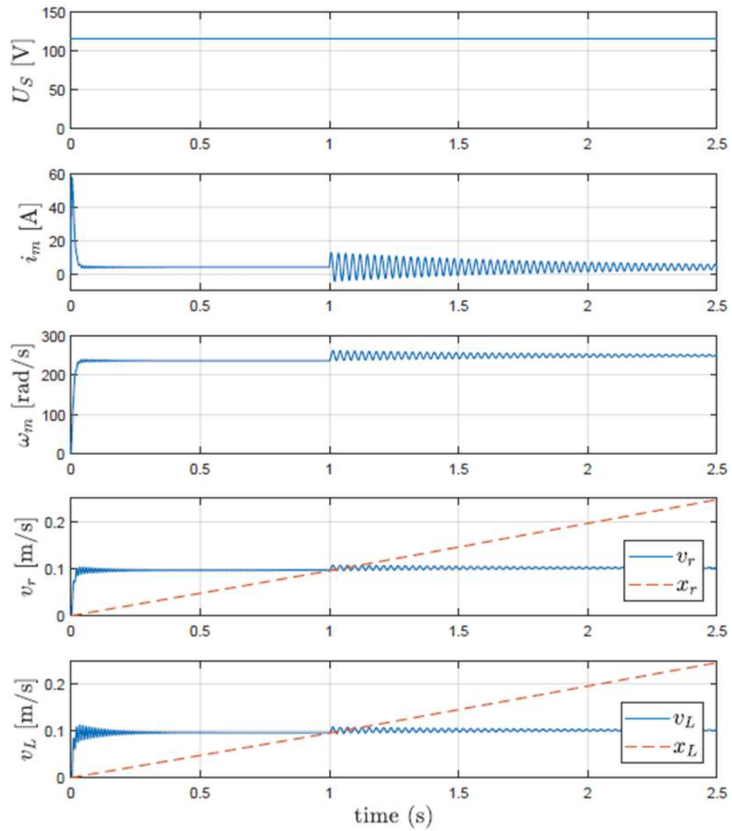

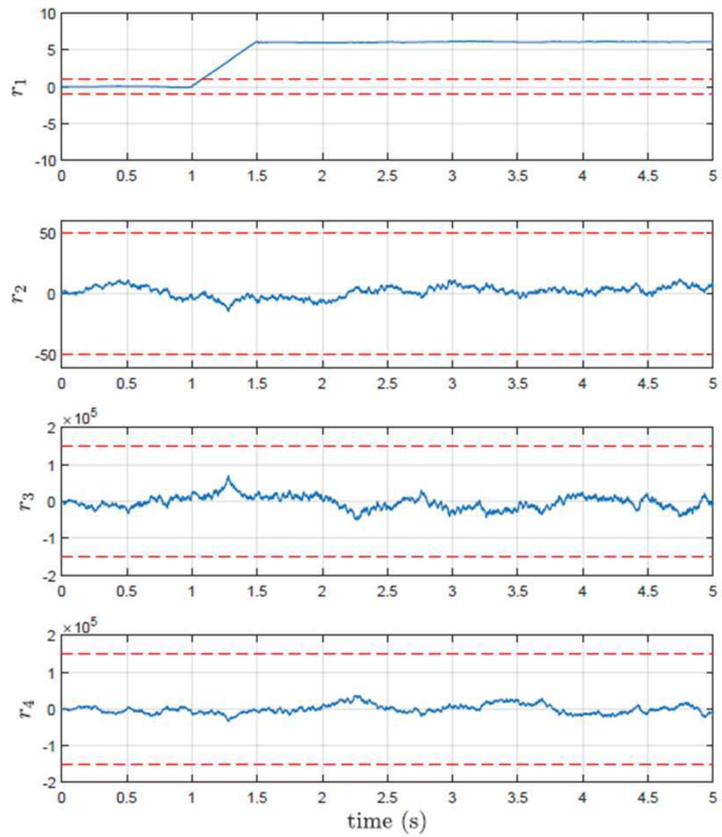

SHORT-CIRCUIT

Subsystem	Component	res_1	res_2	res_3	res_4	D	I
EM electrical part	U_s	1	0	0	0	1	0
	L_w	1	0	0	0	1	0
	R_w	1	0	0	0	1	0
EM mechanical part	K_m	1	1	0	0	1	0
	J_m	0	1	0	0	1	0
	R_{fm}	0	1	0	0	1	0
MPT roller-screw	p	0	1	1	0	1	0
	R_{cr}	0	1	1	0	1	0
	K_{cr}	0	1	1	0	1	0
	M_r	0	0	1	0	1	0
	R_{fr}	0	0	1	0	1	0
Load coupling	R_{cL}	0	0	1	1	1	0
	K_{cL}	0	0	1	1	1	0
Load	M_L	0	0	0	1	1	0
	F_{aer}	0	0	0	1	1	0
Sensors	i_m	1	1	0	0	1	0
	ω_m	1	1	1	0	1	1
	v_r	0	1	1	0	1	0
	v_L	0	0	1	1	1	0

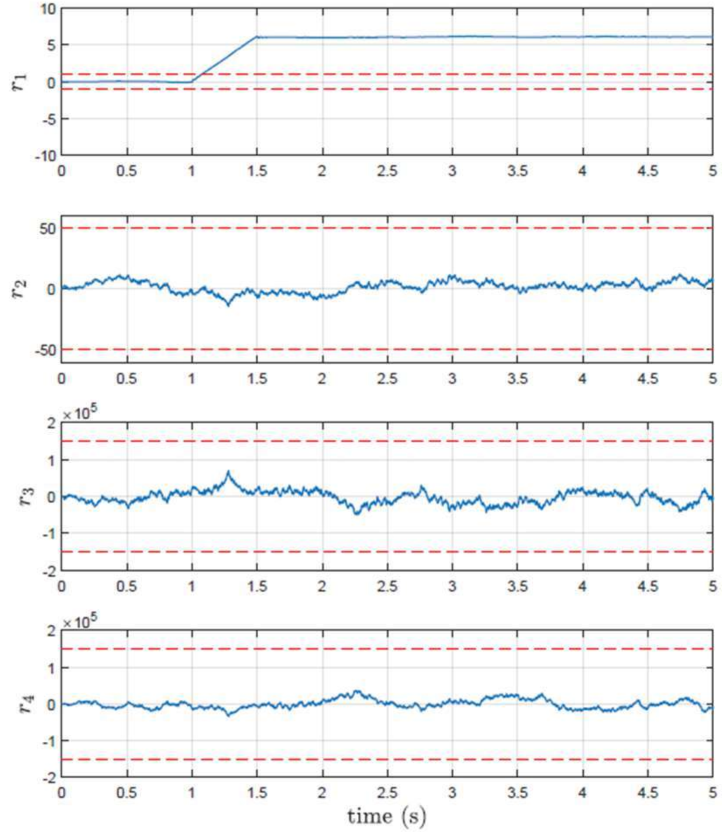

BACKLASH

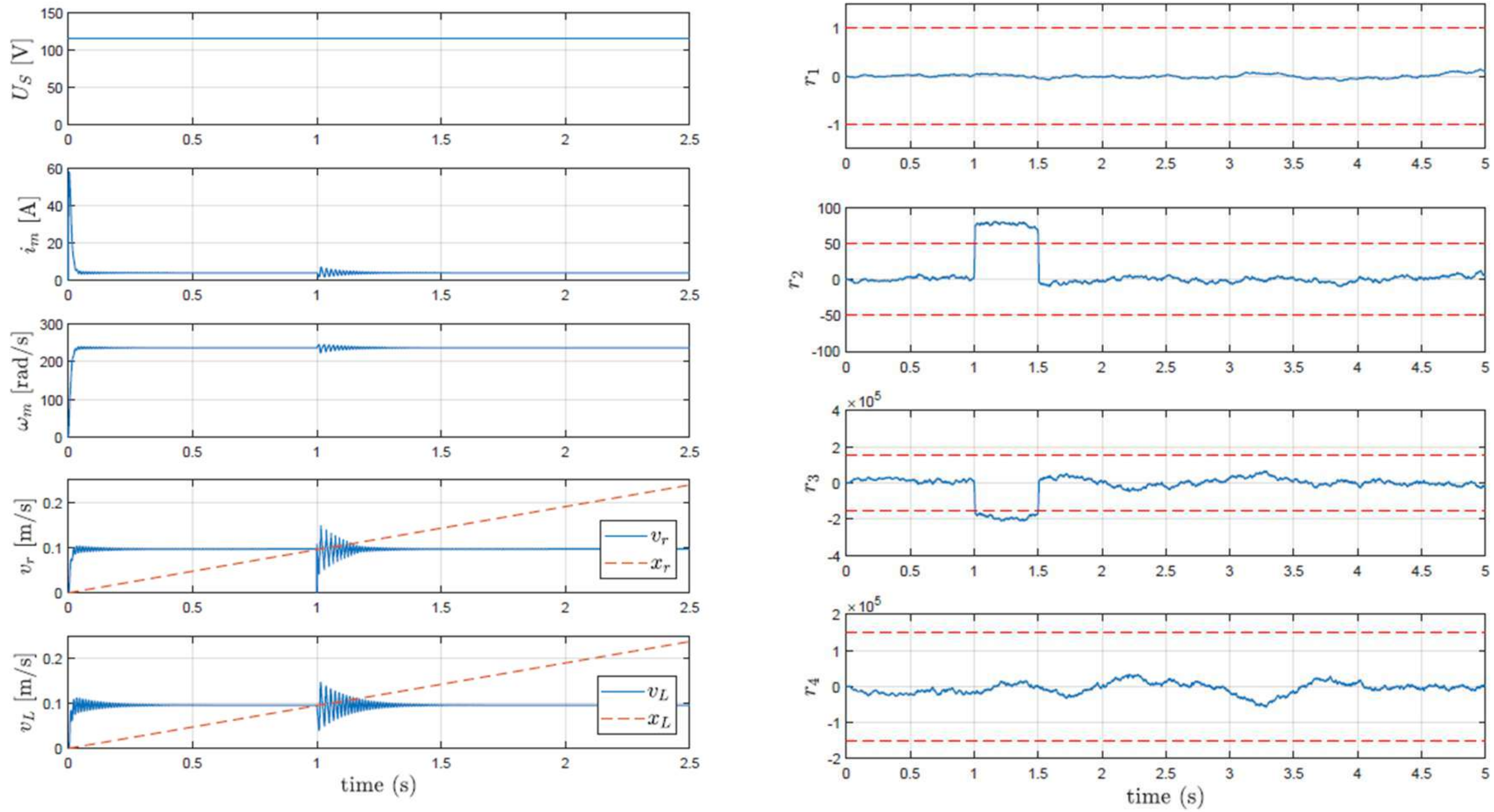

U_S [V]
i_m [A]
ω_m [rad/s]
v_r [m/s]
v_r
x_r
v_L [m/s]
v_L
x_L
time (s)
r_1
r_2
r_3
r_4
$\times 10^5$
time (s)

BACKLASH

Subsystem	Component	res_1	res_2	res_3	res_4	D	I
EM electrical part	U_s	1	0	0	0	1	0
	L_w	1	0	0	0	1	0
	R_w	1	0	0	0	1	0
EM mechanical part	K_m	1	1	0	0	1	0
	J_m	0	1	0	0	1	0
	R_{fm}	0	1	0	0	1	0
MPT roller-screw	p	0	1	1	0	1	0
	R_{cr}	0	1	1	0	1	0
	K_{cr}	0	1	1	0	1	0
	M_r	0	0	1	0	1	0
	R_{fr}	0	0	1	0	1	0
Load coupling	R_{cL}	0	0	1	1	1	0
	K_{cL}	0	0	1	1	1	0
Load	M_L	0	0	0	1	1	0
	F_{aer}	0	0	0	1	1	0
Sensors	i_m	1	1	0	0	1	0
	ω_m	1	1	1	0	1	1
	v_r	0	1	1	0	1	0
	v_L	0	0	1	1	1	0

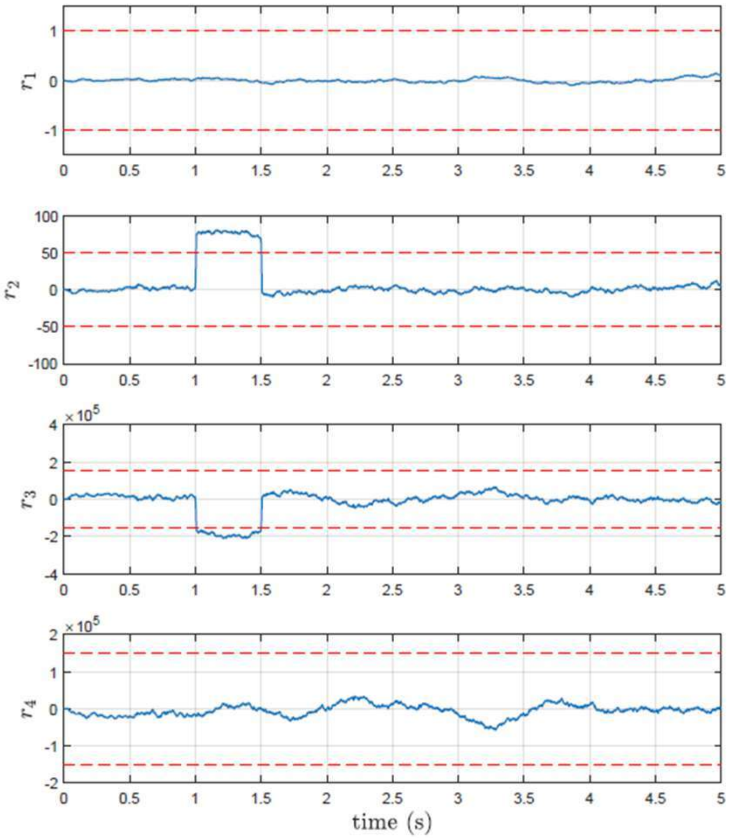

FDI RESULTS SUMMARY

Fault	Fault Injection	Coherence Vector	Fault Candidates
Normal operation	-	$[0,0,0,0]$	-
Open-circuit	R_w	$[1,0,0,0]$	U_s, L_w, R_w
Short-circuit	R_w	$[1,0,0,0]$	U_s, L_w, R_w
Backlash	R_{cr}, K_{cr}	$[0,1,1,0]$	p, R_{cr}, K_{cr}, v_r
Jamming	R_{fr}	$[0,0,1,0]$	M_r, R_{fr}
Mechanical disconnection	R_{cL}, K_{cL}	$[0,0,1,1]$	R_{cL}, K_{cL}, v_L

CONCLUSIONS

The Diagnostic Bond Graph approach was proven as a powerful tool, suitable for the implementation of FDI on complex multidisciplinary systems, such as the electromechanical actuator.

THANK YOU

Gabriel Sobral
gasan.sobral@gmail.com

BIBLIOGRAPHY

BALABAN, E.; SAXENA, A.; BANSAL, P.; GOEBEL, K. F.; STOELTING, P.; CURRAN, S. A diagnostic approach for electro-mechanical actuators in aerospace systems. In: IEEE AEROSPACE CONFERENCE, 2009, Big Sky. **Proceedings [...]**. Piscataway: IEEE, 2009. p. 1-13.

BORUTZKY, W. **Bond graph methodology:** development and analysis of multidisciplinary dynamic system models. London: Springer, 2010. 662p.

FU, J.; MARÉ, J. C.; YU, L.; FU, Y. Multi-level virtual prototyping of electromechanical actuation system for more electric aircraft. **Chinese Journal of Aeronautics**, v. 31, n. 5, p. 892–913, 2018.

QIAO, G.; LIU, G.; SHI, Z.; WANG, Y.; MA, S.; LIM, T. C. A review of electromechanical actuators for More/All Electric aircraft systems. **Proceedings of the Institution of Mechanical Engineers, Part C:** Journal of Mechanical Engineering Science, 2017.

SAMANTARAY, A. K.; BOUAMAMA, B. O. **Model-based process supervision:** a bond graph approach. London: Springer, 2008. 471 p.

EMA MODEL – ELECTRIC MOTOR

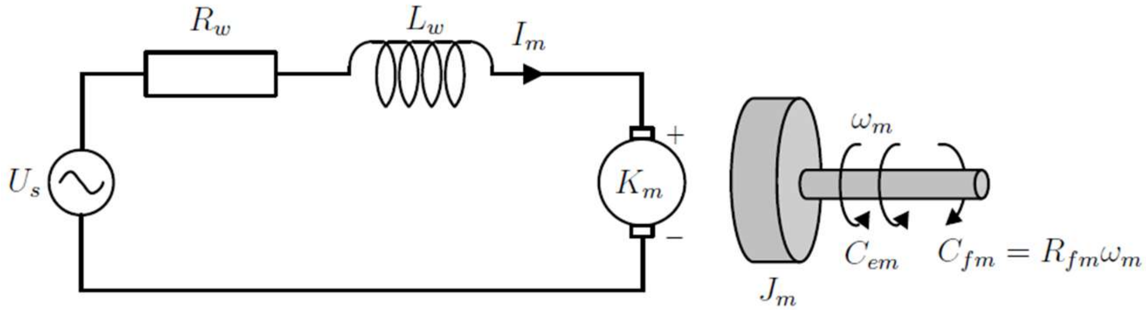

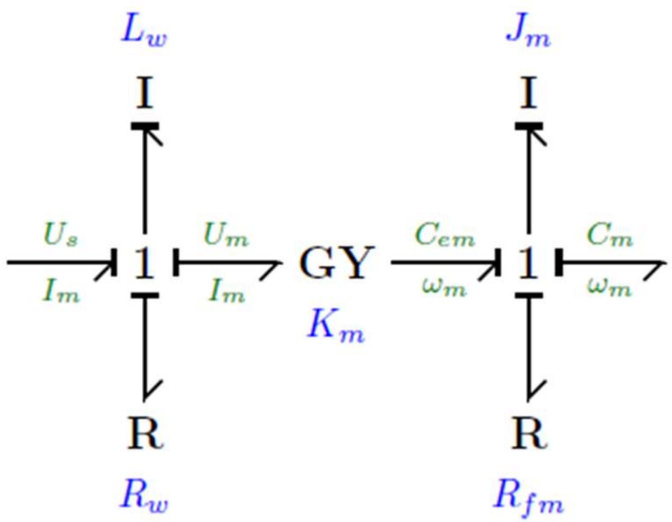

$$C_{em} = I_m K_m$$
$$\omega_m = U_m / K_m$$

EMA MODEL – MECHANICAL POWER TRANSMISSION

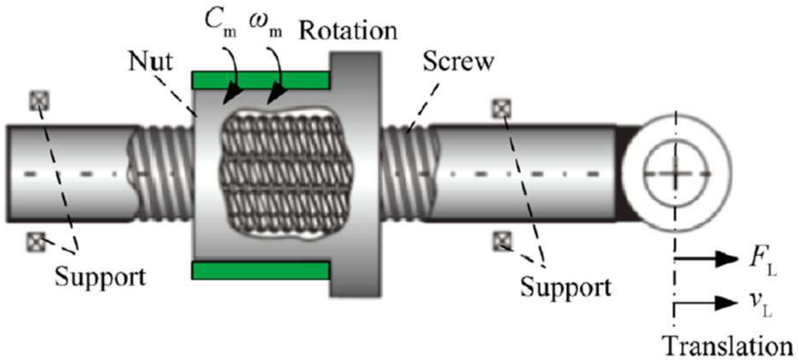

$$F_{ns} = C_m 2\pi/p$$
$$v_{ns} = \omega_m p/2\pi$$

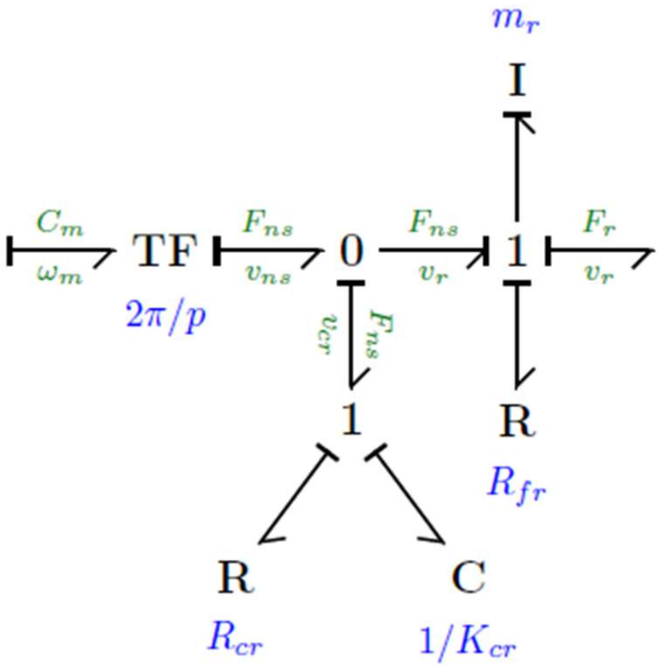

EMA MODEL – LOAD COUPLING

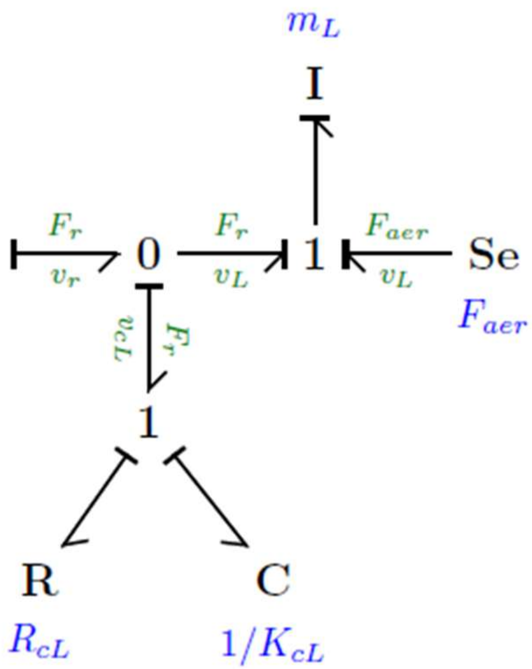

EMA FAULT SIGNATURE MATRIX

Subsystem	Component	res_1	res_2	res_3	res_4	D	I
EM electrical part	U_s	1	0	0	0	1	0
	L_w	1	0	0	0	1	0
	R_w	1	0	0	0	1	0
EM mechanical part	K_m	1	1	0	0	1	0
	J_m	0	1	0	0	1	0
	R_{fm}	0	1	0	0	1	0
MPT roller-screw	p	0	1	1	0	1	0
	R_{cr}	0	1	1	0	1	0
	K_{cr}	0	1	1	0	1	0
	M_r	0	0	1	0	1	0
	R_{fr}	0	0	1	0	1	0
Load coupling	R_{cL}	0	0	1	1	1	0
	K_{cL}	0	0	1	1	1	0
Load	M_L	0	0	0	1	1	0
	F_{aer}	0	0	0	1	1	0
Sensors	i_m	1	1	0	0	1	0
	ω_m	1	1	1	0	1	1
	v_r	0	1	1	0	1	0
	v_L	0	0	1	1	1	0

- Analysis of the causal paths leading to each residual detector
- Detectability index (D) of a component is set to 1 if at least one residual is sensitive to it
- Isolability index (I) is set to 1 when the component's fault signature is different from fault signatures of all other components

EMA FAULT SIGNATURE MATRIX

Subsystem	Component	res_1	res_2	res_3	res_4	D	I
EM electrical part	U_s	1	0	0	0	1	0
	L_w	1	0	0	0	1	0
	R_w	1	0	0	0	1	0
EM mechanical part	K_m	1	1	0	0	1	0
	J_m	0	1	0	0	1	0
	R_{fm}	0	1	0	0	1	0
MPT roller-screw	p	0	1	1	0	1	0
	R_{cr}	0	1	1	0	1	0
	K_{cr}	0	1	1	0	1	0
	M_r	0	0	1	0	1	0
	R_{fr}	0	0	1	0	1	0
Load coupling	R_{cL}	0	0	1	1	1	0
	K_{cL}	0	0	1	1	1	0
Load	M_L	0	0	0	1	1	0
	F_{aer}	0	0	0	1	1	0
Sensors	i_m	1	1	0	0	1	0
	ω_m	1	1	1	0	1	1
	v_r	0	1	1	0	1	0
	v_L	0	0	1	1	1	0

- Analysis of the causal paths leading to each residual detector
- Detectability index (D) of a component is set to 1 if at least one residual is sensitive to it
- Isolability index (I) is set to 1 when the component's fault signature is different from fault signatures of all other components

EMA FAULT SIGNATURE MATRIX

Subsystem	Component	res_1	res_2	res_3	res_4	D	I
EM electrical part	U_s	1	0	0	0	1	0
	L_w	1	0	0	0	1	0
	R_w	1	0	0	0	1	0
EM mechanical part	K_m	1	1	0	0	1	0
	J_m	0	1	0	0	1	0
	R_{fm}	0	1	0	0	1	0
MPT roller-screw	p	0	1	1	0	1	0
	R_{cr}	0	1	1	0	1	0
	K_{cr}	0	1	1	0	1	0
	M_r	0	0	1	0	1	0
	R_{fr}	0	0	1	0	1	0
Load coupling	R_{cL}	0	0	1	1	1	0
	K_{cL}	0	0	1	1	1	0
Load	M_L	0	0	0	1	1	0
	F_{aer}	0	0	0	1	1	0
Sensors	i_m	1	1	0	0	1	0
	ω_m	1	1	1	0	1	1
	v_r	0	1	1	0	1	0
	v_L	0	0	1	1	1	0

- Analysis of the causal paths leading to each residual detector
- Detectability index (D) of a component is set to 1 if at least one residual is sensitive to it
- Isolability index (I) is set to 1 when the component's fault signature is different from fault signatures of all other components

OPEN-CIRCUIT

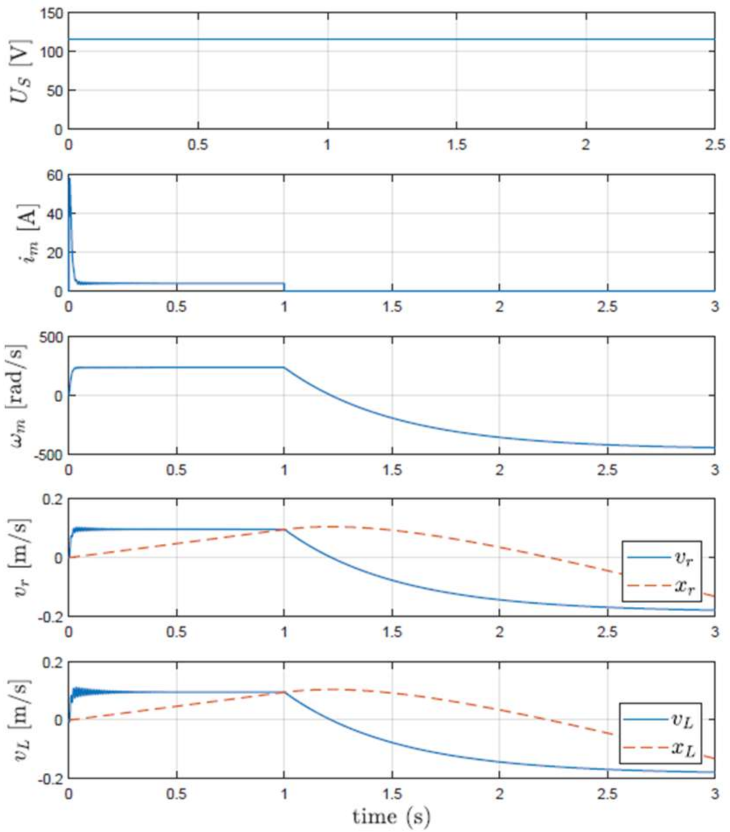

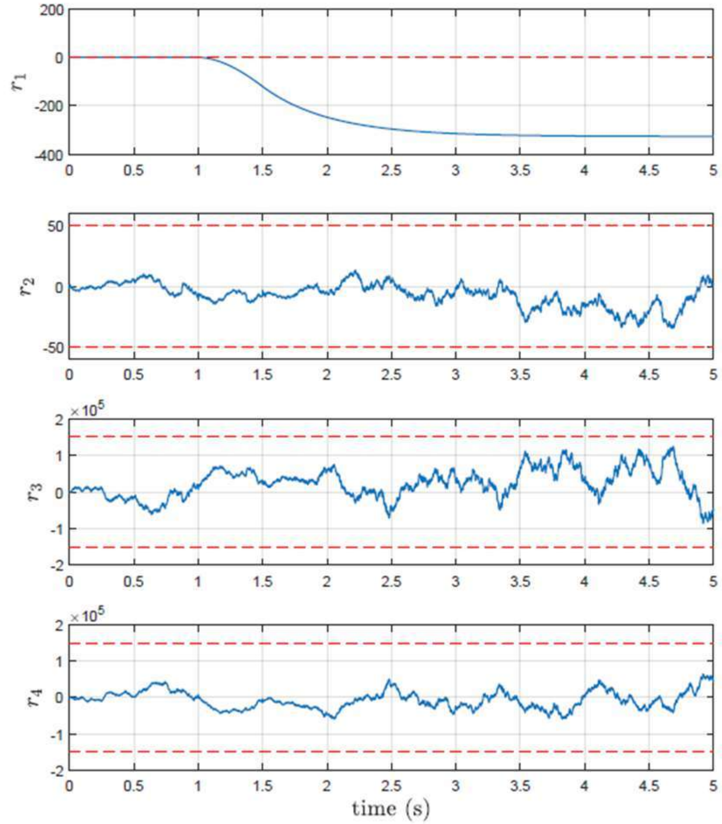

OPEN-CIRCUIT

Subsystem	Component	res_1	res_2	res_3	res_4	D	I
EM electrical part	U_s	1	0	0	0	1	0
	L_w	1	0	0	0	1	0
	R_w	1	0	0	0	1	0
EM mechanical part	K_m	1	1	0	0	1	0
	J_m	0	1	0	0	1	0
	R_{fm}	0	1	0	0	1	0
MPT roller-screw	p	0	1	1	0	1	0
	R_{cr}	0	1	1	0	1	0
	K_{cr}	0	1	1	0	1	0
	M_r	0	0	1	0	1	0
	R_{fr}	0	0	1	0	1	0
Load coupling	R_{cL}	0	0	1	1	1	0
	K_{cL}	0	0	1	1	1	0
Load	M_L	0	0	0	1	1	0
	F_{aer}	0	0	0	1	1	0
Sensors	i_m	1	1	0	0	1	0
	ω_m	1	1	1	0	1	1
	v_r	0	1	1	0	1	0
	v_L	0	0	1	1	1	0

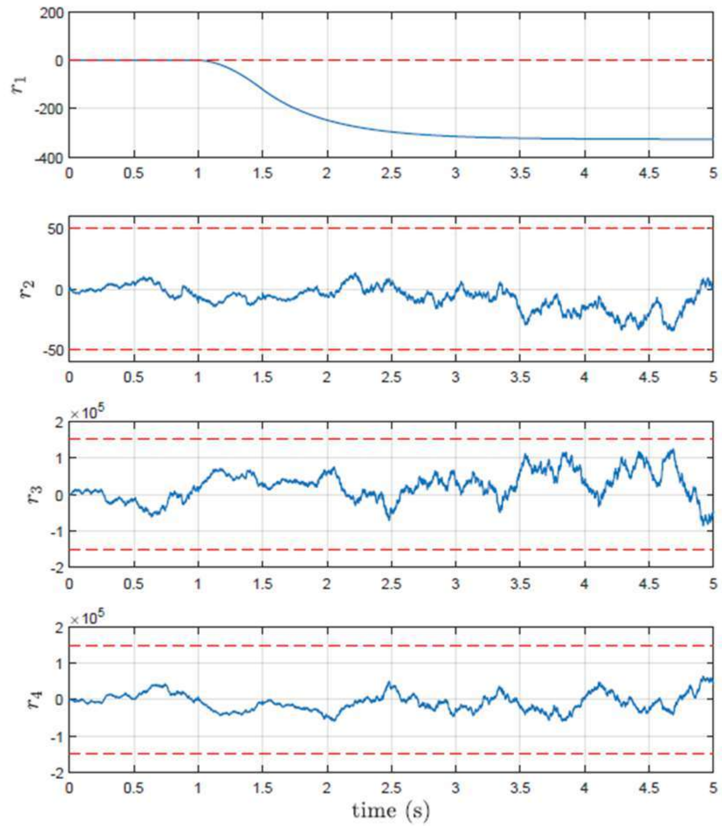

FREE-PLAY

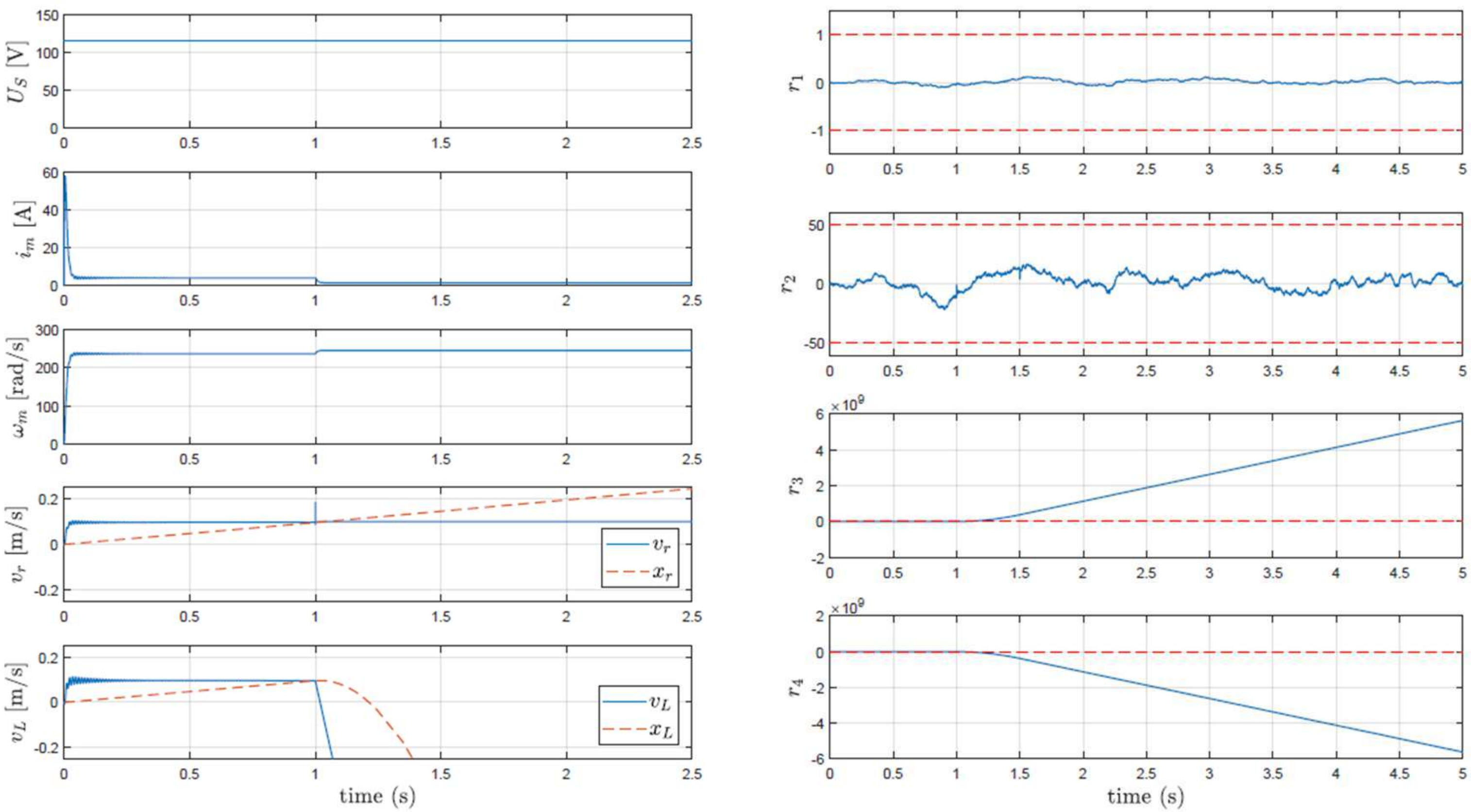

U_S [V]
i_m [A]
ω_m [rad/s]
v_r [m/s]
v_r
x_r
v_L [m/s]
v_L
x_L
time (s)
r_1
r_2
r_3
$\times 10^9$
r_4
$\times 10^9$
time (s)

FREE-PLAY

Subsystem	Component	res_1	res_2	res_3	res_4	D	I
EM electrical part	U_s	1	0	0	0	1	0
	L_w	1	0	0	0	1	0
	R_w	1	0	0	0	1	0
EM mechanical part	K_m	1	1	0	0	1	0
	J_m	0	1	0	0	1	0
	R_{fm}	0	1	0	0	1	0
MPT roller-screw	p	0	1	1	0	1	0
	R_{cr}	0	1	1	0	1	0
	K_{cr}	0	1	1	0	1	0
	M_r	0	0	1	0	1	0
	R_{fr}	0	0	1	0	1	0
Load coupling	R_{cL}	0	0	1	1	1	0
	K_{cL}	0	0	1	1	1	0
Load	M_L	0	0	0	1	1	0
	F_{aer}	0	0	0	1	1	0
Sensors	i_m	1	1	0	0	1	0
	ω_m	1	1	1	0	1	1
	v_r	0	1	1	0	1	0
	v_L	0	0	1	1	1	0

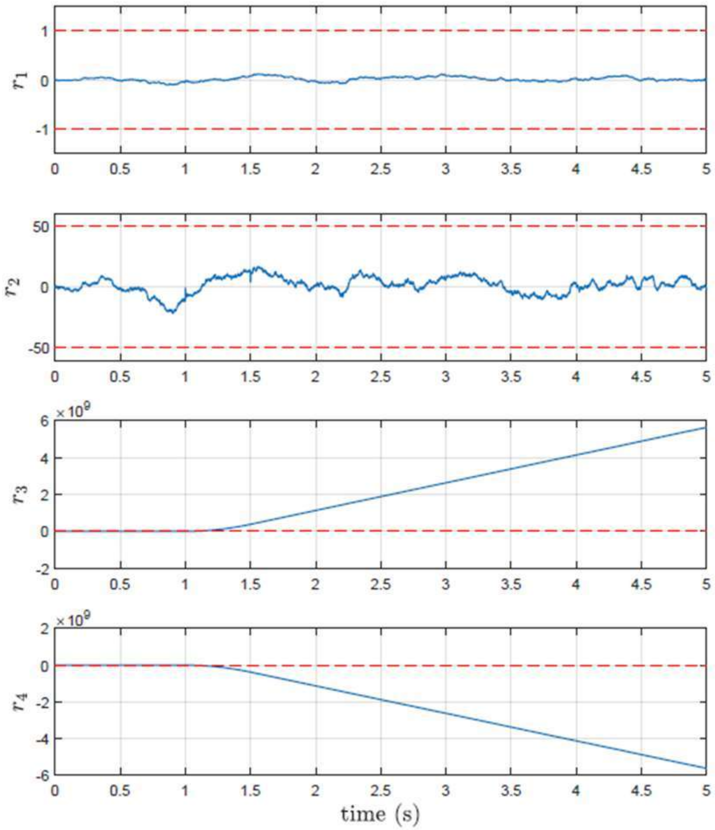

JAMMING

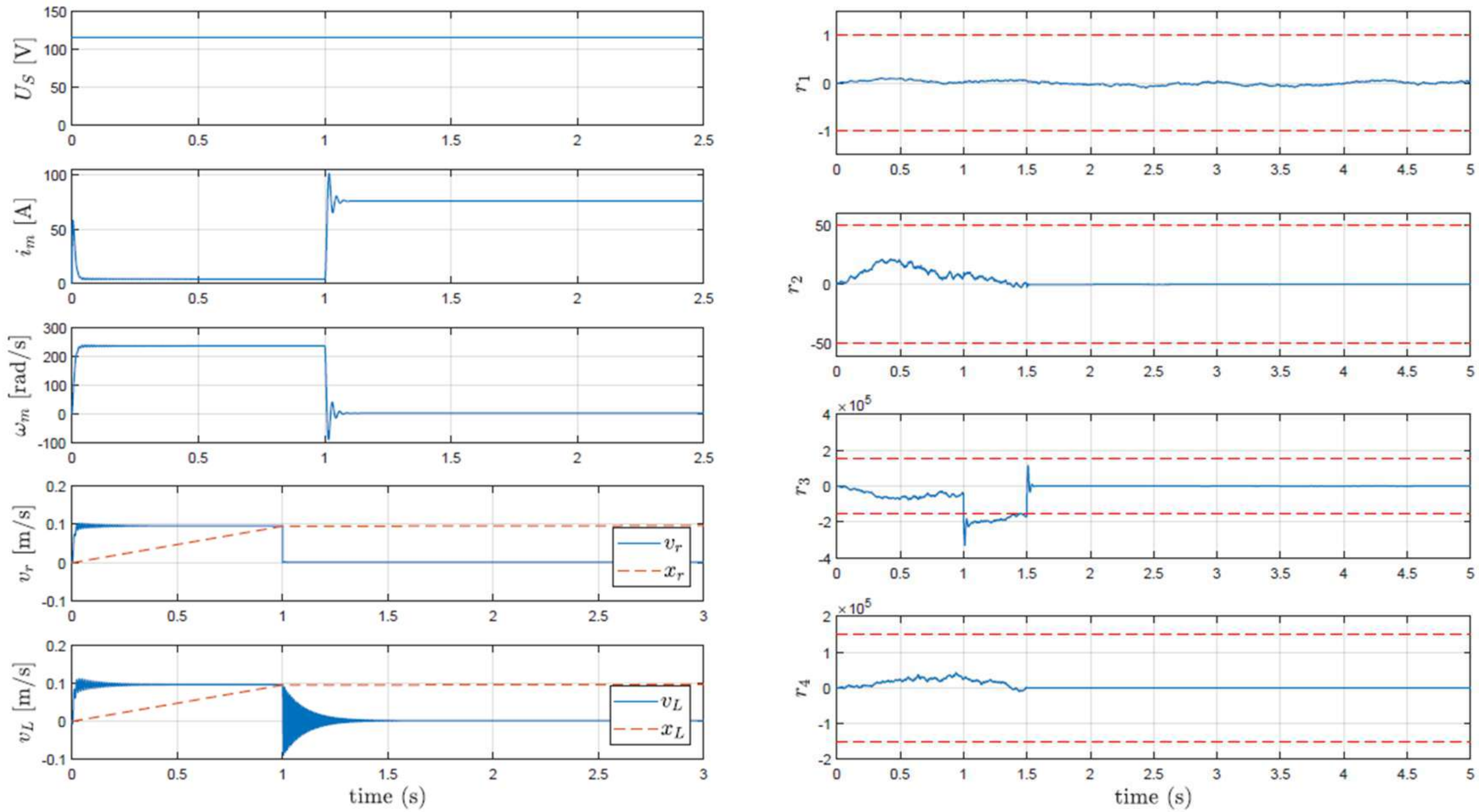
U_S [V]
i_m [A]
ω_m [rad/s]
v_r [m/s]
v_r
x_r
v_L [m/s]
v_L
x_L
time (s)
r_1
r_2
r_3
$\times 10^5$
r_4
$\times 10^5$
time (s)

JAMMING

Subsystem	Component	res_1	res_2	res_3	res_4	D	I
EM electrical part	U_s	1	0	0	0	1	0
	L_w	1	0	0	0	1	0
	R_w	1	0	0	0	1	0
EM mechanical part	K_m	1	1	0	0	1	0
	J_m	0	1	0	0	1	0
	R_{fm}	0	1	0	0	1	0
MPT roller-screw	p	0	1	1	0	1	0
	R_{cr}	0	1	1	0	1	0
	K_{cr}	0	1	1	0	1	0
	M_r	0	0	1	0	1	0
	R_{fr}	0	0	1	0	1	0
Load coupling	R_{cL}	0	0	1	1	1	0
	K_{cL}	0	0	1	1	1	0
Load	M_L	0	0	0	1	1	0
	F_{aer}	0	0	0	1	1	0
Sensors	i_m	1	1	0	0	1	0
	ω_m	1	1	1	0	1	1
	v_r	0	1	1	0	1	0
	v_L	0	0	1	1	1	0

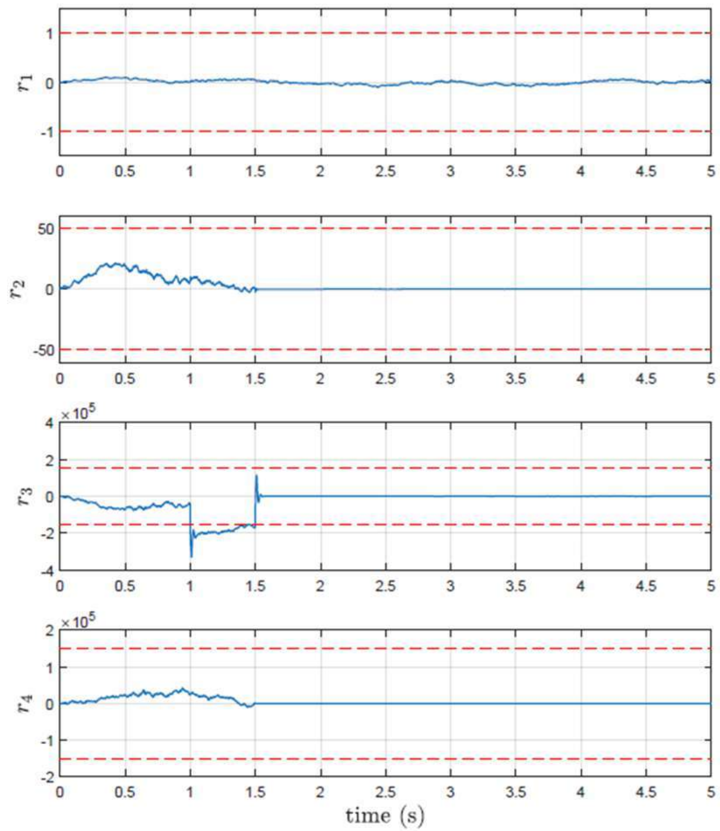

FUTURE RESEARCH

1. Refinement of the EMA model, including PDE and actuator control;
2. Analysis of the closed loop response, and its impacts over the response to failure modes;
3. Robust FDI and sensitivity analysis of the residuals in the presence of parameter uncertainties;
4. Evaluate the inclusion of more sensors in order to improve faults isolability;
5. Bicausal Bond Graph (BBG) models for analysis and improvement of sensor placement for better isolability;
6. Multiple-fault scenarios, applying multiple-fault isolation techniques;
7. Fault Tolerant Control (FTC) techniques for fault accommodation / passivation;
8. DBG online simulation, with inputs from a real system.

MORE ELECTRIC AIRCRAFT

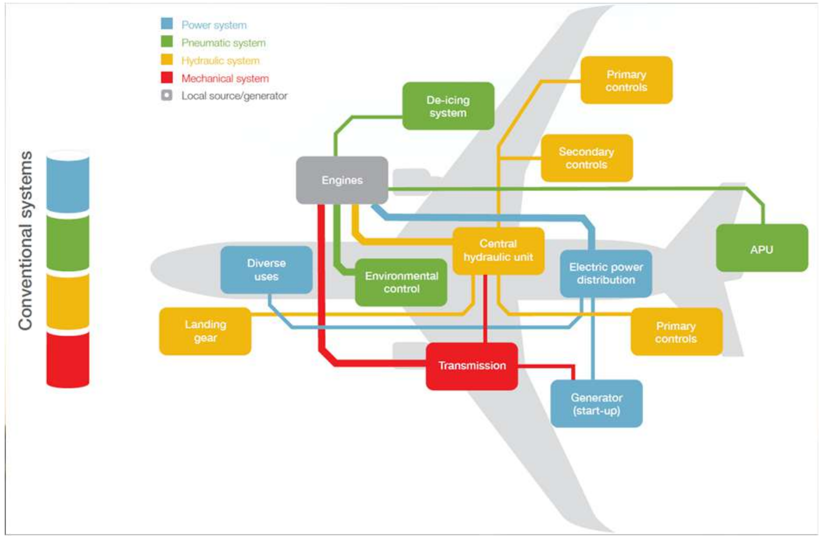

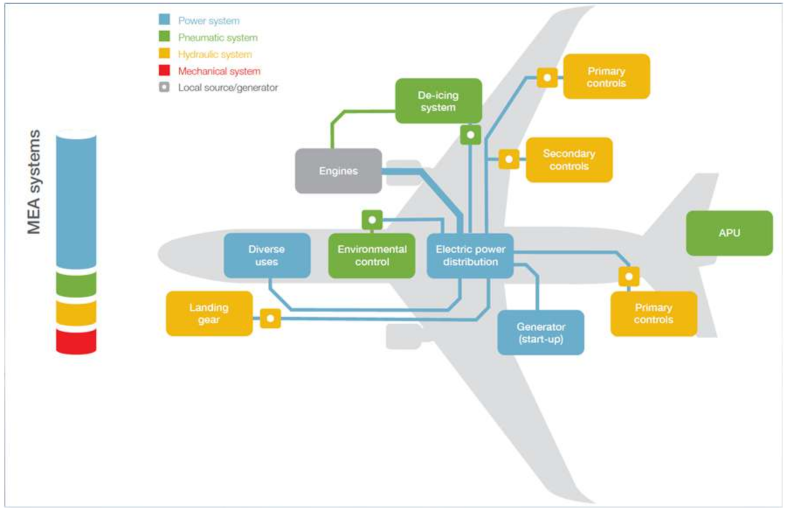

MEA

EMA MODEL PARAMETERS

TABLE 6.1 – EMA model parameters.

Parameter	Value	Unity	Description
J_m	0.001 279	$\mathrm{kg\,m^2\,rad^{-1}}$	EM rotor inertia
K_{cL}	3×10^8	$\mathrm{N\,m^{-1}}$	Load compliance stiffness
K_{cr}	3×10^8	$\mathrm{N\,m^{-1}}$	Roller-Screw compliance stiffness
L_w	3	mH	EM stator winding inductance
M_L	600	kg	Load reflected mass
M_r	1	kg	Roller-screw rod mass
p	2.54	mm	Lead of roller-screw
R_{cL}	1×10^4	$\mathrm{N\,s\,m^{-1}}$	Load compliance damping
R_{cr}	1×10^4	$\mathrm{N\,s\,m^{-1}}$	Roller-screw compliance damping
R_{fm}	1×10^{-3}	$\mathrm{N\,s\,m^{-1}}$	EM friction coefficient
R_{fr}	1×10^4	$\mathrm{N\,s\,m^{-1}}$	Roller-screw friction coefficient
K_m	0.46	$\mathrm{N\,m\,A^{-1}}$	EM torque constant
R_w	1.5	Ω	EM stator winding resistance
U_s	115	V	Bus voltage

Source: (EXLAR, 2018; FU *et al.*, 2016; WANG; MARÉ, 2014).

CAUSAL PATH ANALYSIS

Causal paths leading to residual r1:

1. $\mathbf{U_s} \rightarrow e_1 \rightarrow e_{23} \rightarrow e_{24} \rightarrow \mathbf{res_1}$
2. $\mathbf{i_m} \rightarrow f_{25} \rightarrow f_{23} \rightarrow f_2 \rightarrow \mathbf{L_w} \rightarrow e_2 \rightarrow e_{23} \rightarrow e_{24} \rightarrow \mathbf{res_1}$
3. $\omega_\mathbf{m} \rightarrow f_{28} \rightarrow f_{26} \rightarrow f_5 \rightarrow \mathbf{K_m} \rightarrow e_4 \rightarrow e_{23} \rightarrow e_{24} \rightarrow \mathbf{res_1}$
4. $\mathbf{i_m} \rightarrow f_{25} \rightarrow f_{23} \rightarrow f_3 \rightarrow \mathbf{R_w} \rightarrow e_3 \rightarrow e_{23} \rightarrow e_{24} \rightarrow \mathbf{res_1}$

$$\mathrm{res}_1(U_s, i_m, L_w, \omega_m, K_m, R_w)$$

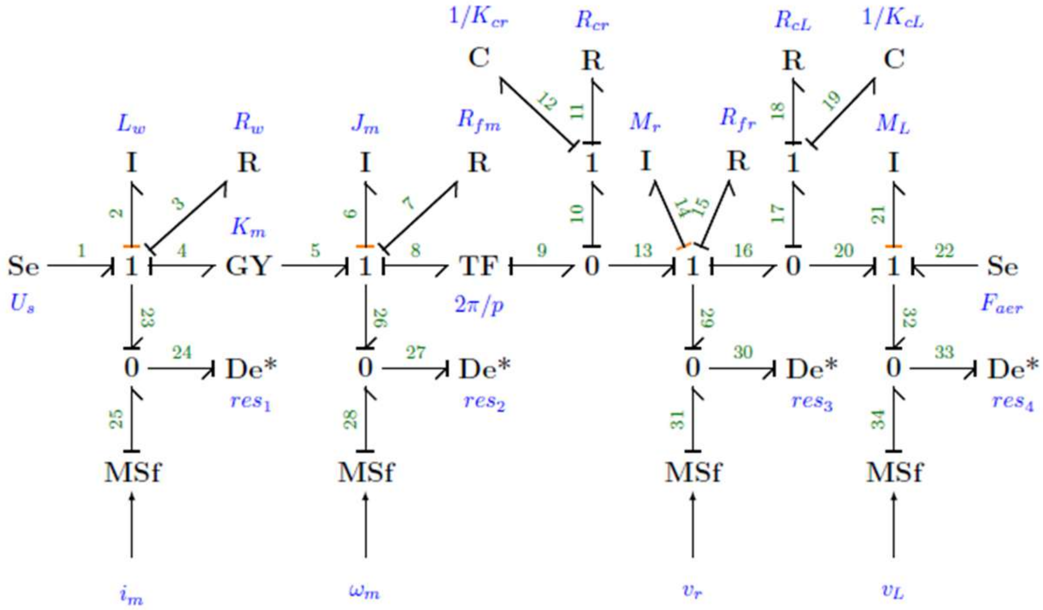

FIGURE 5.9 – EMA diagnostic bond graph model.

BACKLASH MODEL

Pure spring effect: using $x_0 = 0$, the elastic force F_e is purely proportional to the relative displacement x_e and is given by equation 5.10

$$F_e = k_e x_e \tag{5.10}$$

Backlash effect: using $x_0 > 0$, configures a dead zone ($F_e = 0$) of $2x_0$ and the elastic force F_e is given by equation 5.11

$$F_e = \begin{cases} k_e(x_e - x_0) & x_e > x_0 \\ 0 & |x_e| \leq x_0 \\ k_e(x_e + x_0) & x_e < -x_0 \end{cases} \tag{5.11}$$

Preload effect: using $x_0 < 0$, configures a preload force $|F_0| = k_e|x_0|$ and the elastic force F_e is given by equation 5.12

$$F_e = \begin{cases} k_e(x_e - x_0) & x_e > -x_0 \\ 2k_e x_e & |x_e| \leq |x_0| \\ k_e(x_e + x_0) & x_e < x_0 \end{cases} \tag{5.12}$$

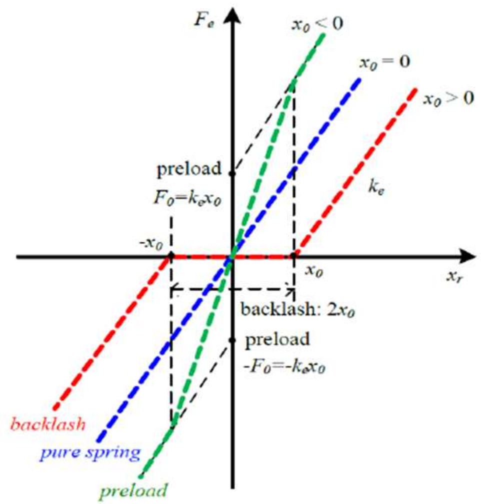

FIGURE 5.7 – Compliance model with backlash and preload effects (FU *et al.*, 2016).

EXPERIMENTAL THRESHOLDS

TABLE 6.2 – Experimental residual thresholds, using 0.5 s moving average.

Residual (r_i)	Threshold (ε_i)
r_1	1
r_2	50
r_3	$1.5e5$
r_4	$1.5e5$

NOISE MODEL

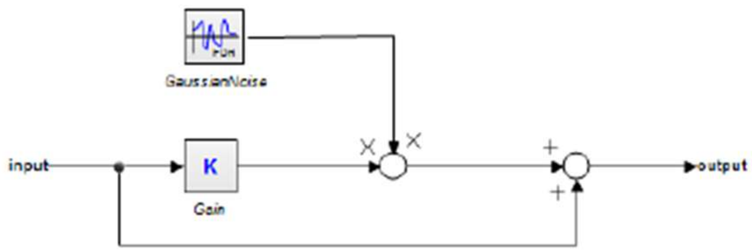

FIGURE 6.9 – 20-sim implementation of the noise model.